Gao *et al. Horticulture Advances* (2024) 2:28
https://doi.org/10.1007/s44281-024-00051-6

Horticulture Advances

RESEARCH ARTICLE Open Access

Integrative DNA methylome and transcriptome analysis illuminate leaf phenotype alterations in tetraploid citrus

Hu Gao[1], Gong-Ao Xiao[1], Yi Bao[1], Qiang-Ming Xia[1], Kai-Dong Xie[1], Xiao-Meng Wu[1*] and Wen-Wu Guo[1,2*]

Abstract

Whole-genome duplication (WGD) in plants triggers profound morphological and physiological changes, with DNA modification being a key epigenetic factor that helps neo-polyploids overcome challenges and gain adaptive advantages. Tetraploids were previously mined from diploid citrus seedlings, showing enhanced environmental adaptability and potential as rootstocks. These tetraploids exhibited increased leaf and cell wall thickness compared to their diploid counterparts. To explore the impact of WGD, transcriptomic and whole-genome bisulfite sequencing (WGBS) were conducted on two pairs of citrus tetraploids and their diploid controls, revealing significant molecular changes. Notably, tetraploid citrus displayed lower CG methylation levels in gene and transposable element (TE) bodies relative to diploids. Differentially methylated genes (DMGs) between tetraploids and diploids were primarily associated with immune stress, organ development, metabolic pathways, and secondary metabolism. In Trifoliate orange (*Poncirus trifoliata* L. Raf.) and Ziyang Xiangcheng (*Citrus junos Sieb*. ex Tanaka), only 150 and 58 differentially expressed genes (DEGs) were identified, respectively, with enrichment in critical cellular processes such as cell wall synthesis, plastid development, and pathways modulating chloroplasts and plasma membranes. A total of 70 genes showed both differential methylation and expression, including *ACN1*, *Nac036*, and *ASMT1*, which are involved in stomatal development, leaf morphology, and melatonin synthesis, respectively, offering insight into the regulatory mechanisms of phenotype alterations after polyploidization. These findings reveal the epigenetic modifications in polyploid citrus and highlight the role of polyploidization-induced methylation in driving phenotypic changes.

Keywords Citrus, Polyploid, DNA methylation, Transcriptome, DMG

Introduction

Polyploidy, including whole-genome duplication (WGD), is a crucial mechanism driving the evolution and diversification of flowering plants (Soltis et al. 2014). Many essential crops, such as wheat, cotton, and oilseed rape, are allopolyploids, while others like alfalfa and potato are autopolyploids. Compared to diploids, polyploids often display significant morphological and physiological changes, such as accelerated growth, enlarged cells, tissues, and organs, as well as metabolic shifts and enhanced resilience to environmental stresses (Lavania et al. 2012). In the early stages of polyploid evolution, newly formed polyploids may face obstacles such as meiotic irregularities, genomic instability, and epigenetic alterations, yet natural polyploid species tend to exhibit greater genomic stability over time (Comai 2005). Epigenetic modifications are believed to play a pivotal role in both the establishment and long-term stability of polyploid plants.

*Correspondence:
Xiao-Meng Wu
wuxm@mail.hzau.edu.cn
Wen-Wu Guo
guoww@mail.hzau.edu.cn
[1] National Key Laboratory for Germplasm Innovation & Utilization of Horticultural Crops, College of Horticulture and Forestry Sciences, Huazhong Agricultural University, Wuhan 430070, China
[2] Hubei Hongshan Laboratory, Wuhan 430070, China

Springer

© The Author(s) 2024. **Open Access** This article is licensed under a Creative Commons Attribution 4.0 International License, which permits use, sharing, adaptation, distribution and reproduction in any medium or format, as long as you give appropriate credit to the original author(s) and the source, provide a link to the Creative Commons licence, and indicate if changes were made. The images or other third party material in this article are included in the article's Creative Commons licence, unless indicated otherwise in a credit line to the material. If material is not included in the article's Creative Commons licence and your intended use is not permitted by statutory regulation or exceeds the permitted use, you will need to obtain permission directly from the copyright holder. To view a copy of this licence, visit http://creativecommons.org/licenses/by/4.0/.

In plants, DNA methylation occurs in three sequence contexts: CG, CHG, and CHH (with H representing A, T, or C), and two key methylation mechanisms are recognized: *de novo* methylation and maintenance methylation. In Arabidopsis, *de novo* DNA methylation is mediated by the RNA-directed DNA methylation (RdDM) pathway, while the maintenance of CG, CHG, and CHH methylation is governed by distinct enzymes: DNA methyltransferase 1 (MET1) for CG, chromomethylase 3 (CMT3) for CHG, and both RdDM and chromomethylase 2 (CMT2) for CHH methylation (Matzke and Mosher 2014). In the RdDM pathway, 24-nt siRNAs direct *de novo* cytosine methylation, with domains rearranged methylase 2 (DRM2) carrying out methylation across all sequence contexts (Matzke and Mosher 2014). In autotetraploid rice, increased siRNA abundance has been linked to CHG and CHH hypermethylation of class II transposable elements (TEs), subsequently reducing the expression of nearby genes (Zhang et al. 2015). DNA methylation levels are regulated by dynamic methylation and demethylation processes, which influence key molecular pathways in plant development (Finnegan et al. 2000), viral immunity (Pooggin 2013), gene imprinting (Li et al. 1993), transposon silencing (Ibarra et al. 2012), and embryogenesis (Rival et al. 2013). DNA methylation is a critical epigenetic modification that regulates development, stress responses, and genome stability in plants (Zhang et al. 2018).

Citrus, a globally significant fruit crop, has a genome size of approximately 327 Mb (Xu et al. 2013). Tetraploidization frequently occurs in citrus due to the spontaneous doubling of chromosomes in nucellar embryonic cells (Aleza et al. 2011). Tetraploid citrus rootstocks have been shown to demonstrate enhanced tolerance to drought, salinity, and cold compared to diploids (Saleh et al. 2008; Wang et al. 2022; Wei et al. 2019). Furthermore, primary metabolite levels differ between tetraploids and their diploid counterparts, accounting for 11-34% of the metabolites detected, with secondary metabolite levels generally increasing while primary metabolites decline (Tan et al. 2015, 2017). This study examined the leaves of diploid and tetraploid Ziyang Xiangcheng (XC) and Trifoliate orange (TO), two widely used rootstocks in China. Whole-genome bisulfite and transcriptome sequencing were employed to compare gene expression and DNA methylation patterns between diploid and tetraploid citrus, aiming to elucidate the relationship between epigenetic and transcriptomic changes and their impacts on phenotypic alterations in citrus polyploids. This study aims to identify the key genes responsible for the phenotypic modifications following WGD.

Methods and materials

Plant material, chromosome preparation, and transmission electron microscopy

Tetraploids (2n=4x=36) were selected from nucellar seedlings of diploid XC and TO (2n=2x=18) and grown in potted soil within a greenhouse (Liang et al. 2014). Fully expanded spring flush leaves from both tetraploids and diploids were collected from the fourth or fifth segment from the apex and stored at -80°C.

The root tip chromosome squashing procedure was adapted with minor adjustments from a previously established method (Xia et al. 2020). Vigorous root tips were harvested and pre-treated in a saturated dichlorobenzene solution for 3 hours at room temperature, followed by fixation in fresh Carnoy's fixative (ethanol: acetic acid = 3:1, v/v) for 24 hours. Fixed samples were then transferred to 75% ethanol and stored at 4°C. Before slide preparation, the root tips underwent enzymatic digestion using a solution of 1% pectinase (Sigma-Aldrich), 2% cellulase (Onozuka R-10, Yakult), and 1% pectolyase (Y-23, Yakult) at 37°C for 90 minutes. Chromosome spreads were prepared *via* the flame-drying method, and images were captured using a fluorescence microscope (Imager M2, Zeiss, Germany) and ZEN software.

For transmission electron microscopy (TEM), specimens were initially fixed with 25% glutaraldehyde (pH 7.4) and 2% osmium tetroxide. After dehydration, they were embedded in epoxy resin. Ultrathin sections were cut using a UC6 ultramicrotome (Leica, Germany) and then stained with uranyl acetate and citric acid. Imaging was performed using a Hitachi H-7650 TEM (Tokyo, Japan), equipped with a Gatan 832 CCD camera, at an acceleration voltage of 80 kV.

Genome-wide bisulfite sequencing and data analysis

DNA libraries were constructed by Novogene Bioinformatics Technology Co. Ltd (Beijing, China). Raw BS-seq data were filtered using Trimmomatic (Bolger et al. 2014) to remove low-quality reads. High-quality reads were then aligned to reference genomes with BS-Seeker2 (Guo et al. 2013); XC samples were mapped to the *Citrus sinensis* v2.0 genome, while TO samples were aligned to the *Poncirus trifoliata* v1.0 genome (Huang et al. 2021; Wang et al. 2021b). The resulting mapped files were processed using Cgmaptools for methylation analysis and visualized in IGV software (Guo et al. 2018). Differentially methylated regions (DMRs) were identified *via* the Cgmaptools DMR function, using a dynamic fragmentation method with default parameters. A $\Delta mC \geq 0.1$ and a t-test *P*-value ≤ 0.01 were set as the thresholds. The genes with promoter regions (2 kb) or gene bodies overlapping with DMRs were classified as differentially methylated genes (DMGs).

TEs in citrus were identified and annotated using RepeatMasker. To assess methylation levels, upstream and downstream regions of the gene bodies and TEs were divided into 100 bp intervals, and methylation was calculated for each interval to display the distribution of DNA methylation. Functional enrichment analyses of DMGs were performed using Gene Ontology (GO) and Kyoto Encyclopedia of Genes and Genomes (KEGG) pathways (Kanehisa et al. 2008), with KEGG pathway enrichment validated *via* KOBAS (Bu et al. 2021).

RNA sequencing and data analysis

For transcriptome analysis, three biological replicates were prepared by pooling leaves from four individual plants for each replicate. RNA-Seq libraries were constructed by Novogene Bioinformatics Technology Co. Ltd (Beijing, China). After filtering out low-quality reads, adapter sequences, and poly-N sequences, clean reads were obtained and mapped to reference genomes using STAR (Dobin et al. 2013). Transcript abundance was quantified using FeatureCount (Liao et al. 2014), and normalized to Transcripts Per Kilobase Million (TPM). Differential gene expression was analyzed with the DESeq2 R package (Love et al. 2014), defining differentially expressed genes (DEGs) as those with an adjusted *P*-value <0.05 and $|\log2(\text{fold change})| \geq 1$.

Quantitative real-time PCR (RT-PCR) analysis

The HiScript II Q RT SuperMix for qPCR kit (Vazyme) was utilized for reverse transcription of RNA to cDNA. qRT-PCR was performed using the 2X Universal SYBR Green Fast qPCR Mix (ABclonal), with data normalized to *ACT7*. Gene expression levels were quantified using the $2^{-\Delta\Delta Ct}$ method. Primer sequences are listed in Table S1.

Bisulfite sequencing PCR (BS-PCR) analysis

The EZ DNA Methylation-Gold™ Kit (Zymo Research) was employed to convert unmethylated cytosines to thymines, followed by PCR amplification of *PtACN1*. Hi-Tom sequencing (http://www.hi-tom.net/hi-tom/) was used to analyze PCR products, with primers designed *via* Kismeth (https://katahdin.girihlet.com/kismeth/primer_design.pl#) and listed in Table S1.

Small RNA sequencing and data analysis

Library construction and sequencing were carried out by Novogene Bioinformatics Technology Co. Ltd (Beijing, China). Clean reads were obtained by removing adapters, low-quality sequences, and contaminants. Reads shorter than 18 bp or longer than 30 bp were excluded before genome mapping using sRNAminer (Li et al. 2024), and the total number of clean reads was used for read normalization.

Results

Morphological changes in leaves after genome doubling

Significant morphological differences exist between XC and TO leaves. XC leaves are narrow and elongated, with wide, long-winged petioles, whereas TO leaves are trifoliolate. While the morphology of tetraploid leaves resembles that of their diploid counterparts, they are larger and exhibit a deeper green color (Fig. 1a). TEM revealed that tetraploid leaf cell walls were notably thicker compared to diploid leaves (Fig. 1b, Table S2). Chromosome counts confirmed that diploids (XC-2x and TO-2x) have 18 chromosomes, while tetraploids (XC-4x and TO-4x) possess 36 chromosomes (Fig. 1c).

Genome-wide DNA methylation levels of diploid and tetraploid citrus leaves

To explore the potential role of DNA methylation in the phenotypic changes observed during citrus genome doubling, whole-genome bisulfite sequencing (WGBS) was conducted on XC-2x, TO-2x, XC-4x, and TO-4x leaves. After removing adapters and low-quality reads, the average number of clean reads was 89.15 million for diploids and 272.4 million for tetraploids. Following alignment to the *Citrus sinensis* and *Poncirus trifoliata* genomes, 51.52–228.94 million reads were uniquely mapped for each sample, with a mapping rate exceeding 54%. The sequencing depth ranged from 24× to 113×, indicating that cytosine detection reached saturation (Table S3).

Genome-wide methylation levels were assessed across different sequence contexts. In XC diploid and tetraploid, 17.39% and 17.57% of total cytosine sites were methylated, respectively. The average 5mC levels in the CG, CHG, and CHH contexts were 48.22%, 30.88%, and 11.09% in diploids, compared to 47.19%, 30.32%, and 11.48% in tetraploids. For TO, 15.96% and 15.97% of cytosine sites were methylated in diploids and tetraploids, with corresponding 5mC levels of 50.63%, 31.94%, and 8.89% in diploids, and 50.02%, 31.67%, and 8.92% in tetraploids (Fig. 2a, Table S4).

The relative proportions of 5mCs across the three sequence contexts were also calculated. In XC-2x and XC-4x, 26.97% and 26.40% of 5mCs were in CG, 24.16% and 23.61% in CHG, and 48.88% and 49.99% in CHH. For TO-2x and TO-4x, 30.13% and 30.16% were in CG, 26.97% and 26.94% in CHG, and 42.91% and 42.90% in CHH (Fig. 2b, Table S5). XC exhibited higher CHH methylation levels than TO, while TO had greater CG and CHG methylation levels. Analysis of genome-wide methylation in diploids and tetraploids of both XC and TO indicated similar methylation distribution patterns

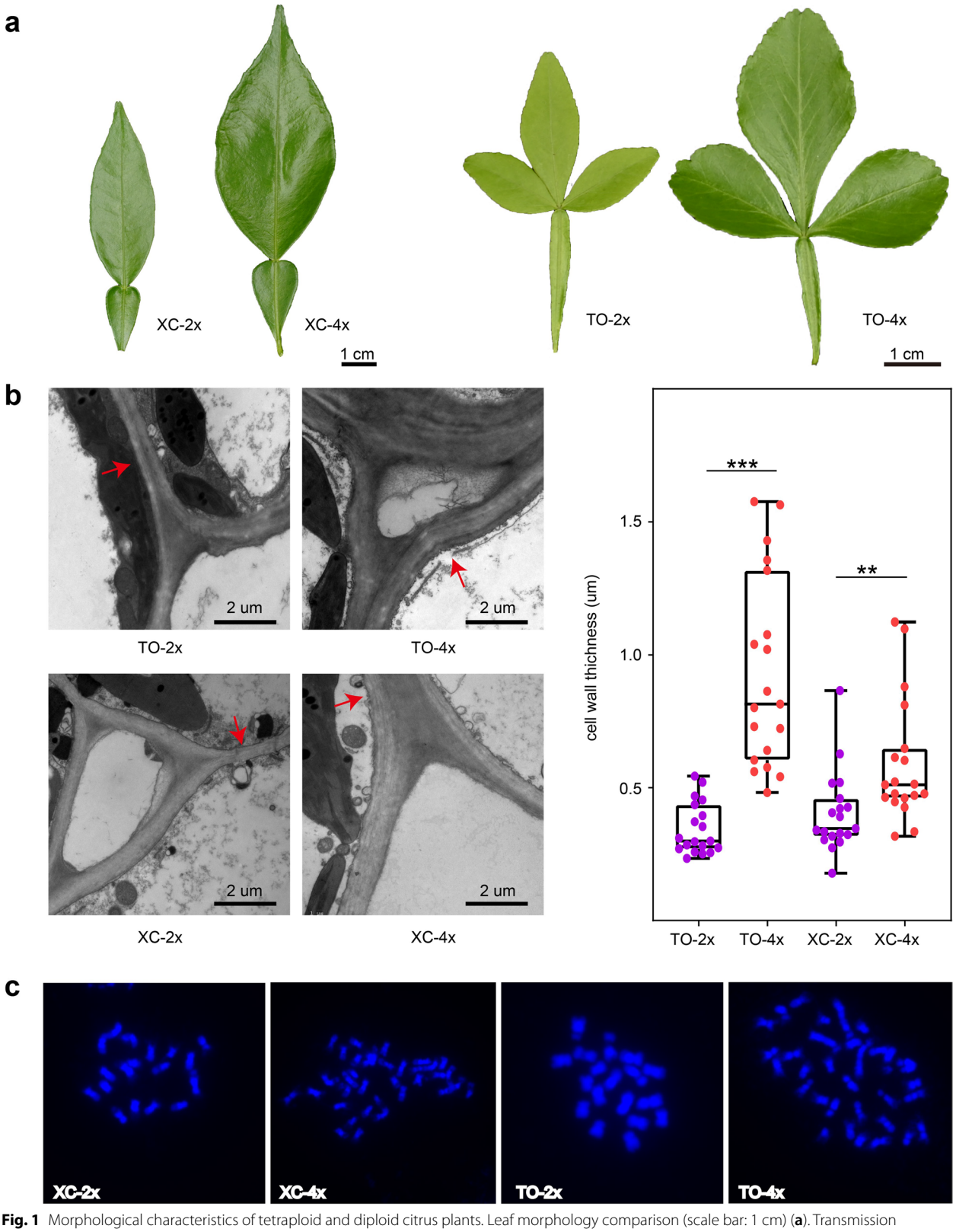


Fig. 1 Morphological characteristics of tetraploid and diploid citrus plants. Leaf morphology comparison (scale bar: 1 cm) (**a**). Transmission electron microscopy of mesophyll cells in diploid (2x) and tetraploid (4x) leaves (scale bar: 2 μm) (**b**). Chromosome counts in diploid (2n=2x=18) and tetraploid (2n=4x=36) root tips (**c**). XC: Ziyang Xiangcheng (*Citrus junos Sieb.* ex Tanaka); TO: Trifoliate orange (*Poncirus trifoliata* L. Raf.)

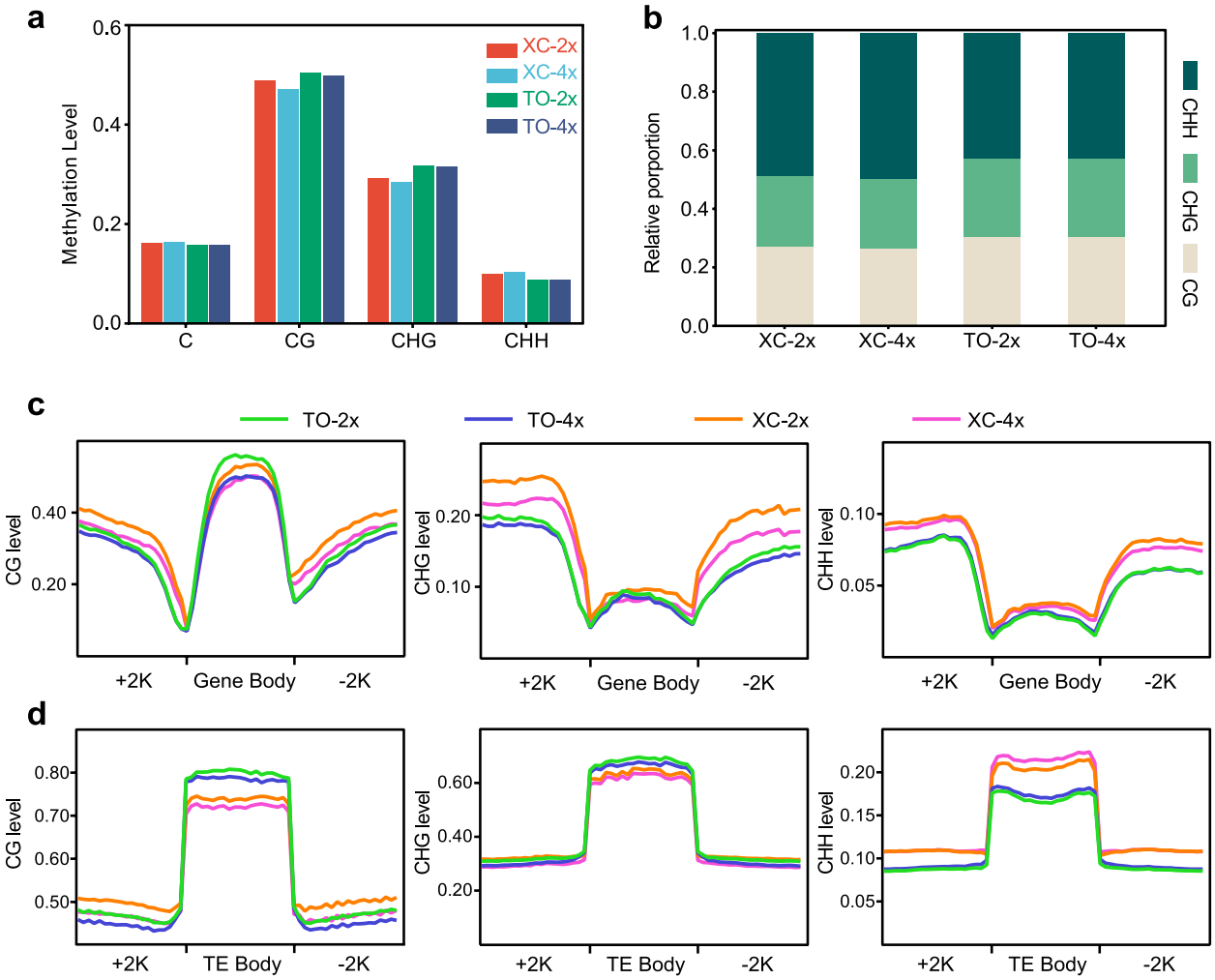


Fig. 2 Global methylome sequencing and DNA methylation profiles in tetraploid and diploid citrus. Proportions of methylated cytosines (mCs) in tetraploid and diploid citrus (**a**). mC ratios in CG, CHG, and CHH contexts (**b**). DNA methylation patterns in gene regions (**c**) and TE regions (**d**). XC: Ziyang Xiangcheng (*Citrus junos Sieb.* ex Tanaka); TO: Trifoliate orange (*Poncirus trifoliata* L. Raf.)

across citrus chromosomes, with higher methylation in TE-enriched regions and lower levels in gene regions (Figures S1 and S2).

DNA methylation pattern in genic and transposable element-rich regions

Methylation levels in the gene body, TE body, and their 2 kb upstream and downstream flanking regions were analyzed to compare diploid and tetraploid citrus. Methylation patterns were largely consistent between diploids and tetraploids within the gene body and flanking regions. CG methylation was elevated in gene regions and reduced in flanking regions, whereas CHG and CHH methylation were higher in the flanking regions but lower in the gene body. Diploids exhibited higher CG methylation within the gene body compared to tetraploids, though differences in CHG and CHH methylation between ploidy levels were less pronounced (Fig. 2c). In TE regions, both diploids and tetraploids displayed similar methylation patterns, with high methylation in TEs and lower levels in flanking regions. However, tetraploids showed increased CHH methylation in TEs, while CG methylation in TEs was lower compared to diploids (Fig. 2d, Table S6).

To elucidate the role of transposons in genome duplication and gene regulation, TEs in the *Citrus sinensis* and *Poncirus trifoliata* genomes were analyzed. Ten of the most abundant transposon superfamilies were identified, including retrotransposons (LTR) such as Copia, Gypsy, Caulimovirus, and LINE, along with DNA transposons like MULE-MuDR, PIF-Harbinger, Helitron, CMC-EnSpm, hAT-Tip100, and hAT-Ac (Fig. 3a, Table S7). Methylation analysis across these transposon superfamilies revealed elevated methylation levels within TE

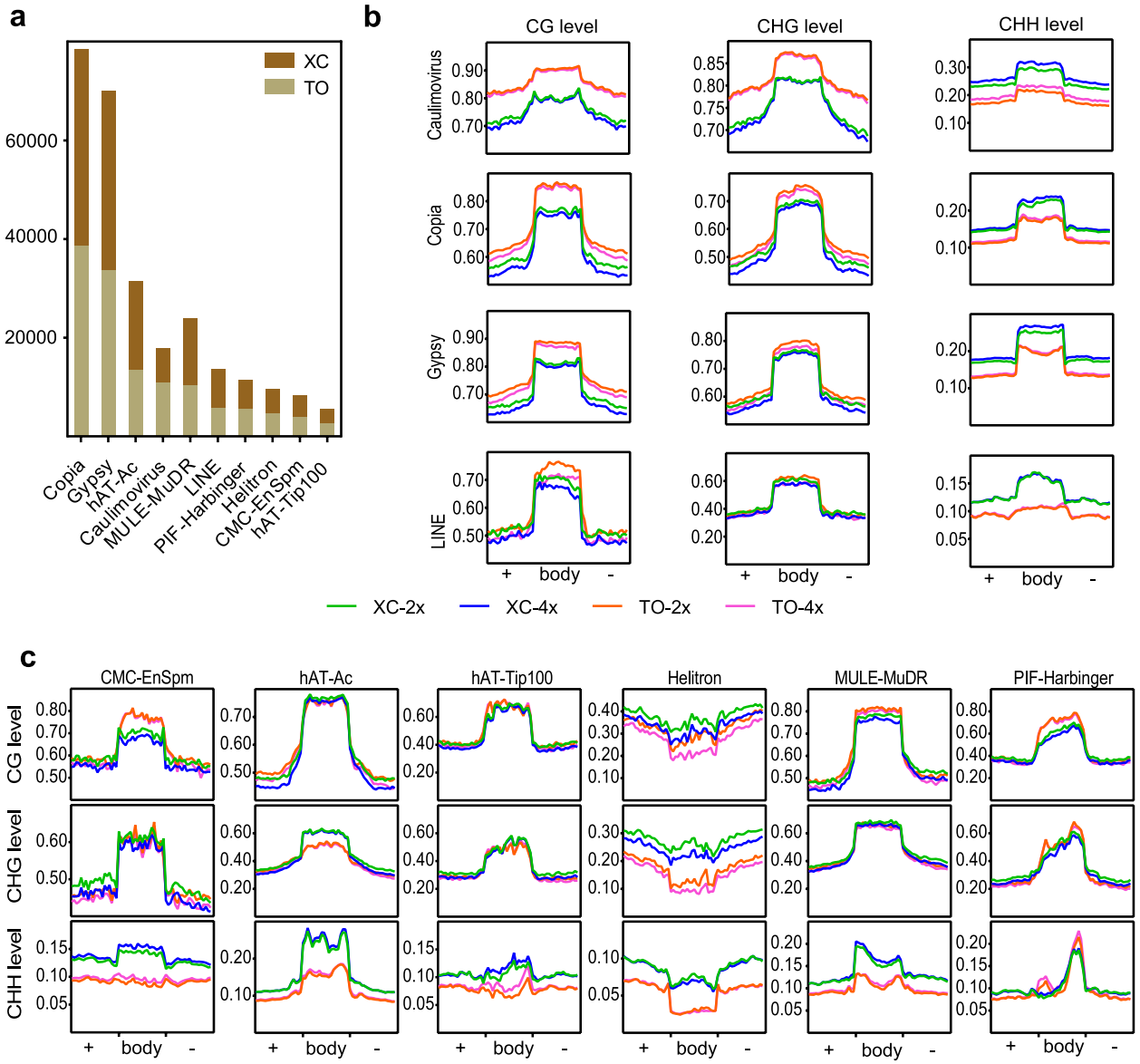


Fig. 3 Average distribution of DNA methylation across various transposable element (TE) types. Types and numbers of TEs identified in Citrus sinensis (dark brown) and *Poncirus trifoliata* (light brown) genomes (**a**). Average DNA methylation distribution in Class I TEs (**b**) and Class II TEs (**c**). XC: Ziyang Xiangcheng (*Citrus junos Sieb.* ex Tanaka); TO: Trifoliate orange (*Poncirus trifoliata* L. Raf.)

regions compared to their flanking regions for all four retrotransposons—Copia, Gypsy, Caulimovirus, and LINE. Notably, in the LINE superfamily, CHH methylation levels showed minimal variation between the TE region and adjacent sequences (Fig. 3b). Except for Helitron, all five DNA transposon superfamilies exhibited uniform methylation patterns in the CG and CHG contexts, with higher methylation within TE regions relative to flanking regions. In the CHH context, methylation distribution varied more significantly across transposon superfamilies (Fig. 3c). Methylation differences between XC and TO were also observed, with TO showing higher CHG methylation in the Copia family, while XC had higher CHG methylation in the hAT-Ac family.

Differentially methylated regions (DMRs) between diploids and tetraploids in citrus

DMRs are recognized as epigenetic biomarkers. A comparison between tetraploid and diploid citrus revealed 2,935 CG-DMRs, 2,670 CHG-DMRs, and 4,794 CHH-DMRs in XC, while TO exhibited 8,697 CG-DMRs, 5,565 CHG-DMRs, and 4,508 CHH-DMRs, with

hypermethylation outnumbering hypomethylation in both cases (Fig. 4a, Table S8). To explore the relationship between DMRs and transposons, the distribution of DMRs within transposon regions was assessed, revealing that a significant proportion (>50%) were located in these regions, aligning with previous reports of transposon methylation during genome doubling (Fig. 4b, Table S9). A detailed analysis of DMR distribution across various genomic features, including 5'UTR, 3'UTR, exons, introns, intergenic, and promoter regions, revealed that DMRs were predominantly located in intergenic regions (Fig. 4c, Table S10). Additionally, the comparison of DMR lengths between XC and TO showed that CHH-DMRs were the longest, while CG-DMRs were the shortest in both species (Fig. 4d).

To determine whether DMGs are conserved after citrus genome doubling, various types of DMGs were quantified between diploids and tetraploids. Statistical and GO enrichment analyses of conserved DMGs between XC and TO highlighted 333 CG-DMGs significantly enriched in immune stress and plant organ development (Fig. 5a, b), 216 CHG-DMGs associated with salicylic acid response and flavonoid biosynthesis (Fig. 5c, d), and 356 CHH-DMGs enriched in responses to fatty acids, jasmonic acid, and plasma membrane development (Fig. 5e, f). These conserved DMGs reflect significant involvement in key biological processes, including immune stress, plant organ development, responses to salicylic and jasmonic acids, and the biosynthesis of flavonoids and fatty acids, along with plasma membrane development.

To further elucidate the biological pathways associated with DMGs, KEGG enrichment analysis was performed. The majority of CG-, CHG-, and CHH-DMGs were enriched in metabolic and secondary metabolic pathways, indicating that DNA methylation changes following genome doubling significantly affect metabolism-related genes in leaves (Figure S3). Additionally, Mapman analysis provided insights into the metabolic processes influenced by DMGs, revealing their roles in various plant hormone signaling pathways, including auxin, brassinosteroid, and abscisic acid, as well as in primary metabolic processes such as lipid metabolism and photorespiration. In secondary metabolism, these DMGs contribute to the synthesis and degradation of phenylpropanoids and play critical roles in reactive

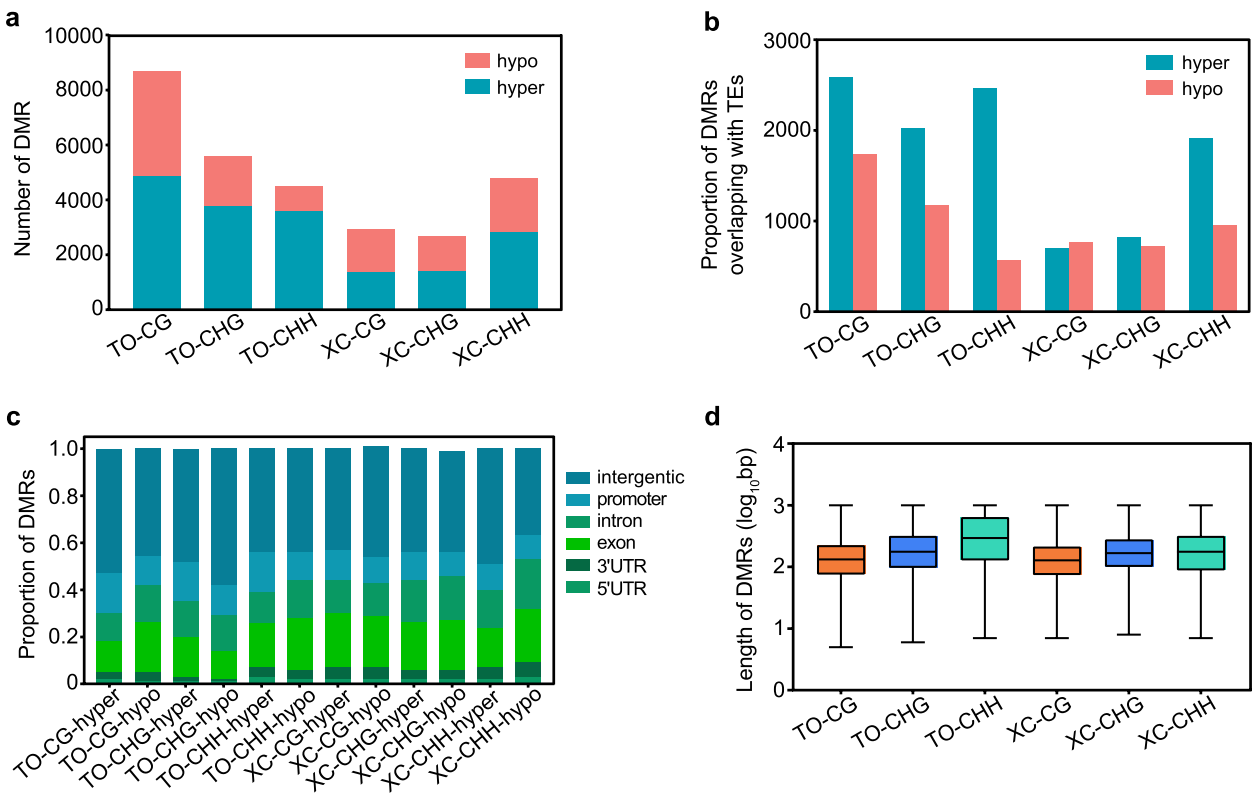


Fig. 4 Analysis of differentially methylated regions (DMRs) between tetraploid and diploid citrus. Counts of hypermethylated and hypomethylated DMRs in CG, CHG, and CHH contexts (**a**). Proportions of hyper- and hypomethylated DMRs overlapping with TEs (**b**). Genome-wide distribution of DMRs (**c**). Length of DMRs in CG, CHG, and CHH contexts (**d**). XC: Ziyang Xiangcheng (*Citrus junos Sieb.* ex Tanaka); TO: Trifoliate orange (*Poncirus trifoliata* L. Raf.)

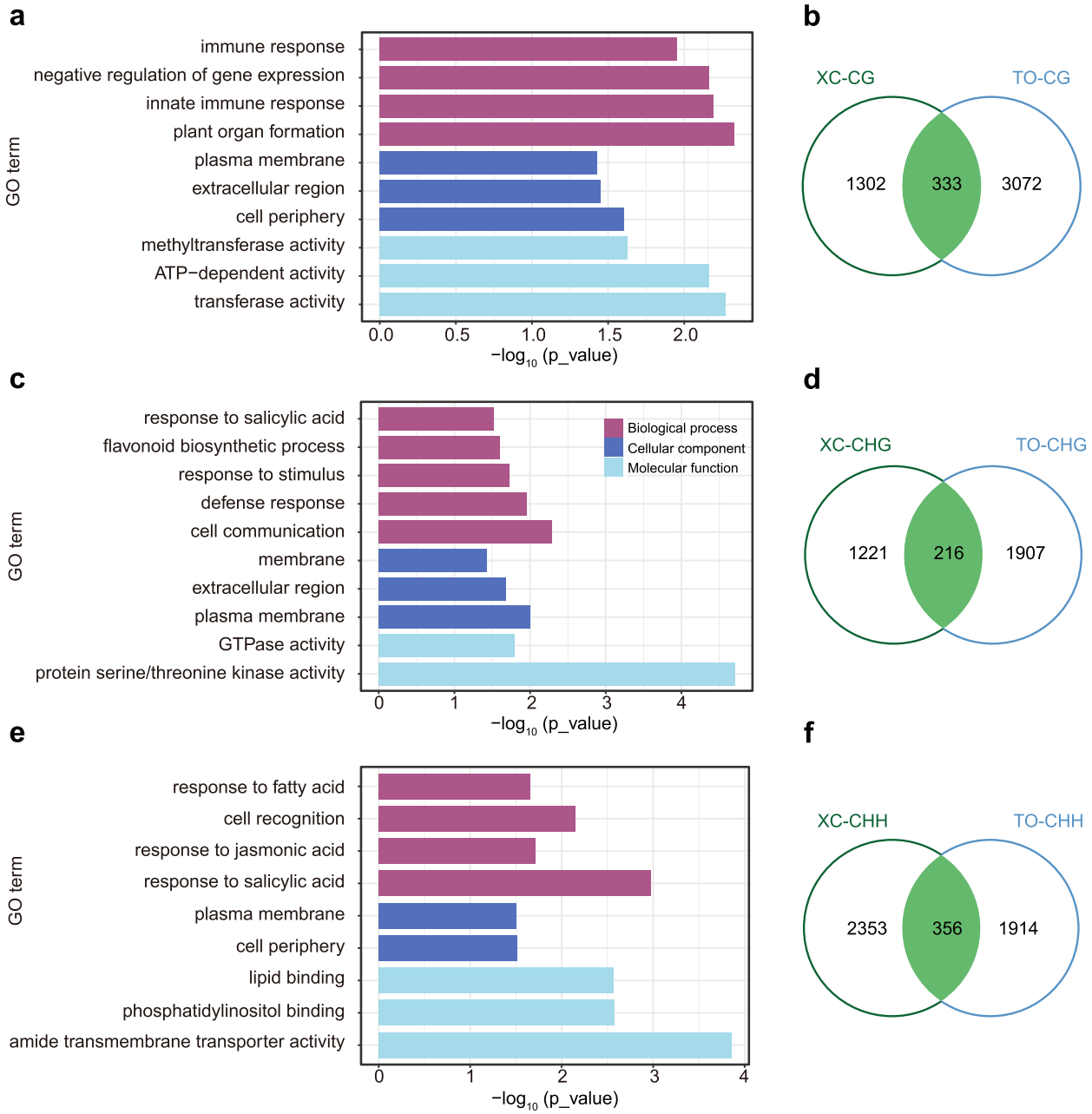


Fig. 5 GO enrichment analysis of differentially methylated regions (DMRs) in CG, CHG, and CHH contexts between tetraploid and diploid citrus conserved in XC and TO. GO enrichment of conserved CG-DMGs (**a**), CHG-DMGs (**c**), and CHH-DMGs (**e**) between tetraploid and diploid conserved in XC and TO. The number of conserved CG-DMGs (**b**), CHG-DMGs (**d**), and CHH-DMGs (**f**) between tetraploid and diploid conserved in XC and TO. XC: Ziyang Xiangcheng (*Citrus junos Sieb.* ex Tanaka); TO: Trifoliate orange (*Poncirus trifoliata* L. Raf.)

oxygen species (ROS)-related responses (Figure S4-S9). The strong enrichment of DMGs in metabolic pathways likely reflects the substantial metabolic differences observed between diploid and tetraploid citrus leaves.

Differentially expressed genes between diploids and tetraploids citrus

To investigate how genome doubling influences gene transcription, a comparative transcriptomic analysis was conducted between diploid and tetraploid leaves. In

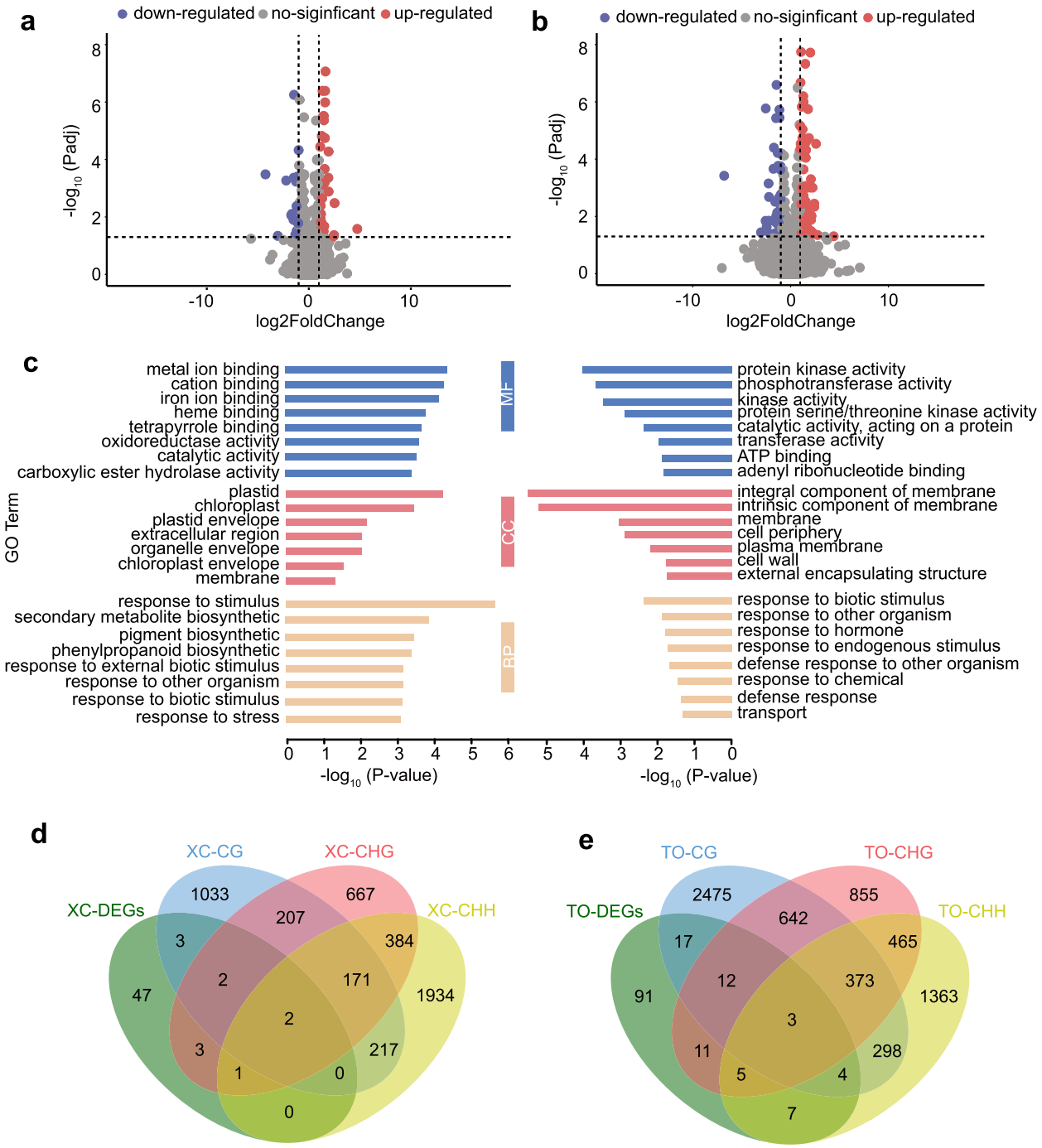


Fig. 6 Differentially expression genes between diploid and tetraploid citrus. Volcano plots showing differentially expressed genes (DEGs) in tetraploid compared to diploid in XC (**a**) and TO (**b**). Red and blue dots represent significantly up- and down-regulated genes, respectively. GO enrichment of DEGs in XC and TO (**c**). Venn diagrams showing the overlap between DMGs in the three contexts and DEGs in XC (**d**) and TO (**e**). XC: Ziyang Xiangcheng (*Citrus junos Sieb.* ex Tanaka); TO: Trifoliate orange (*Poncirus trifoliata* L. Raf.)

XC, 58 DEGs were identified between diploid and tetraploid samples (Fig. 6a), and 150 DEGs were detected in TO (Fig. 6b). The transcriptional profiles displayed minimal variation due to polyploidy in citrus, aligning with previous studies that found fewer than 1% of genes were differentially expressed between tetraploid and diploid citrus varieties, including Rangpur limes and Ziyang xiangcheng (Allario et al. 2011, Tan et al. 2015). DEGs in

both XC and TO were enriched in cellular components such as cell wall biosynthesis, plastid development, and the regulation of chloroplast and plasma membrane composition, as well as in biological processes related to stimulus response, stress response, and hormone response (Fig. 6c). A Venn diagram demonstrated little overlap between DMGs and DEGs, suggesting that methylation changes during genome duplication do not significantly affect gene transcription (Fig. 6d, e).

In comparing tetraploids with diploids, five hypomethylated genes exhibited increased expression, while 42 hypermethylated genes were downregulated (Figure S10). Among the genes showing both altered methylation and transcription, several were identified as potentially contributing to phenotypic differences between diploids and tetraploids, including *CsUGT76B1*, *CsTPS21*, *CsASMT1*, *PtNac036*, and *PtACN1* (Fig. 7a). RT-PCR analysis confirmed that the expression patterns of six DEGs were consistent with RNA-seq results (Figure S11a), with five genes highly expressed in tetraploids and one gene expressed at lower levels. The DNA methylation level of *PtACN1* was validated using BS-PCR, revealing a methylation percentage of 24% in diploids and 45% in tetraploids, consistent with WGBS data showing methylation values of 0.14 in diploids and 0.3 in tetraploids (Figure S11b). These findings confirm that *PtACN1* is more

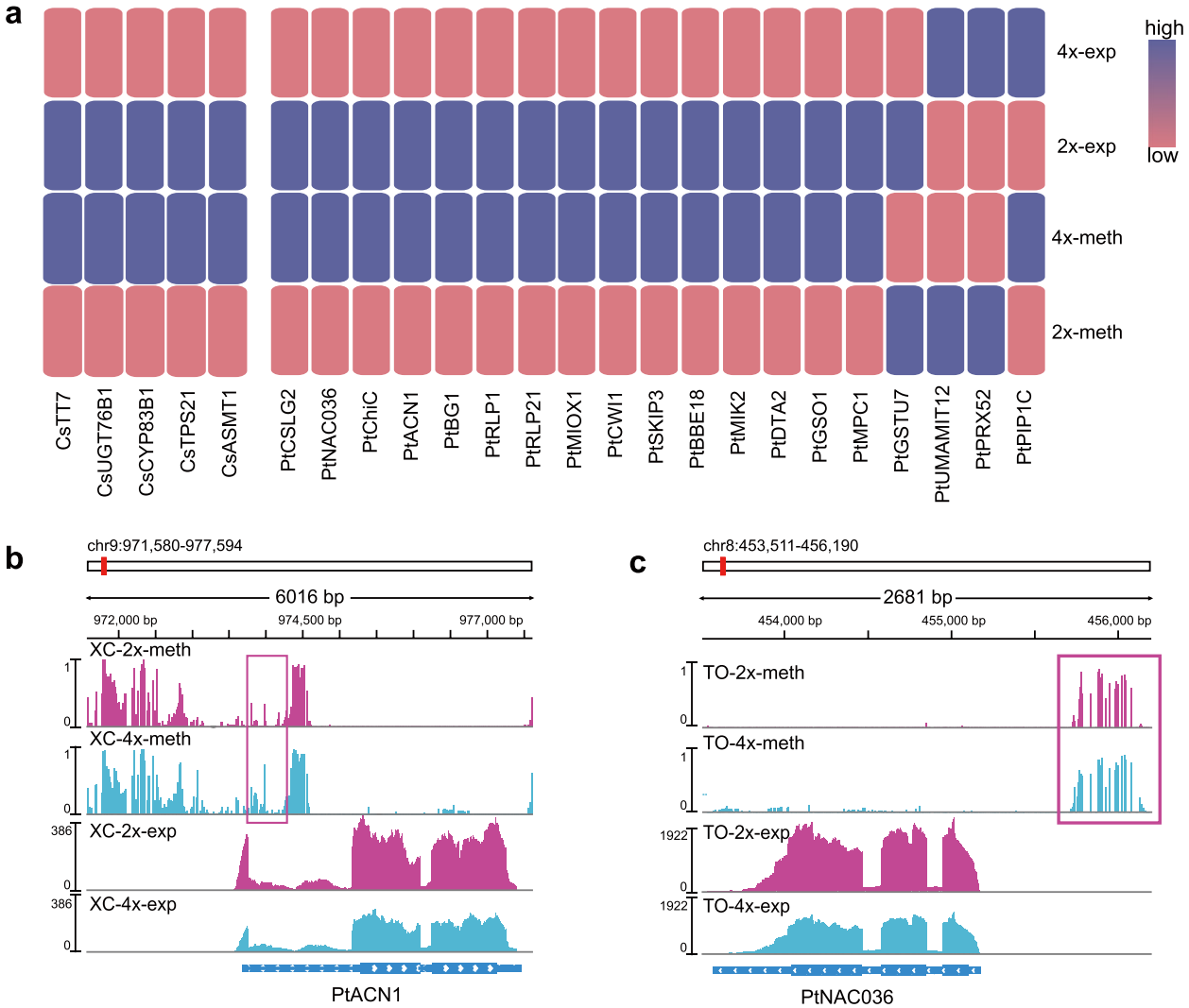


Fig. 7 Integrated analysis of the DNA methylome and transcriptome. Heatmap illustrating genes overlapping between DMGs and DEGs (**a**). IGV snapshots of representative genes *PtACN1* (**b**) and *PtNAC036* (**c**), with both expression and methylation profiles. XC: Ziyang Xiangcheng (*Citrus junos Sieb.* ex Tanaka); TO: Trifoliate orange (*Poncirus trifoliata* L. Raf.). PtACN1: *Poncirus trifoliata ACN1 (ACETATE NON-UTILIZING1)*; PtNAC036: *Poncirus trifoliata NAC036 (NAM, ATAF, and CUC 036)*

highly methylated in tetraploids. *CsUGT76B1* encodes a glycosyltransferase, and the *ugt76b1* mutant in Arabidopsis exhibits reduced plant height and increased disease resistance. *CsTPS21* encodes a sesquiterpene synthase linked to disease resistance. *CsASMT1* encodes cytosolic N-acetylserotonin O-methyltransferase, a rate-limiting enzyme in melatonin synthesis associated with stress response, plant growth, and development. *PtNac036* plays a role in chloroplast development, while *PtACN1* encodes acetyl-coenzyme A synthetase, which modulates drought resistance by controlling guard cell turgor pressure *via* the acetate–malate shunt. These genes offer valuable targets for understanding the molecular mechanisms underlying citrus polyploidization and provide insight into relevant regulatory pathways (Fig. 7b, c).

Effect of 24nt-siRNA on DNA methylation in tetraploids

siRNAs have been implicated in promoting methylation in polyploid plants *via* the RdDM pathway (Zhang et al. 2015). High-throughput sequencing of small RNAs was conducted in both diploid and tetraploid leaves, revealing that among the four samples, 24-nt small RNAs were the most abundant. A notable increase in 24-nt siRNAs was detected in the tetraploid TO sample compared to its diploid counterpart, whereas minimal changes in 24-nt siRNA levels were observed between diploid and tetraploid XC (Figure S12). To assess the relationship between DNA methylation and 24-nt siRNAs, average methylation levels in regions with and without 24-nt siRNAs were examined across XC and TO samples. Methylation in CG, CHG, and CHH contexts was significantly elevated in regions associated with siRNAs compared to those without (Fig. 8a, c). In TO, a greater abundance of 24-nt siRNAs was found in hypermethylated regions of CG, CHG, and CHH than in hypomethylated regions. Conversely, in XC, fewer 24-nt siRNAs were detected in hypermethylated CG regions, while CHG and CHH hypermethylated regions contained higher levels of 24-nt siRNAs than their hypomethylated counterparts (Fig. 8b, d). These findings suggest that 24-nt siRNAs may play a

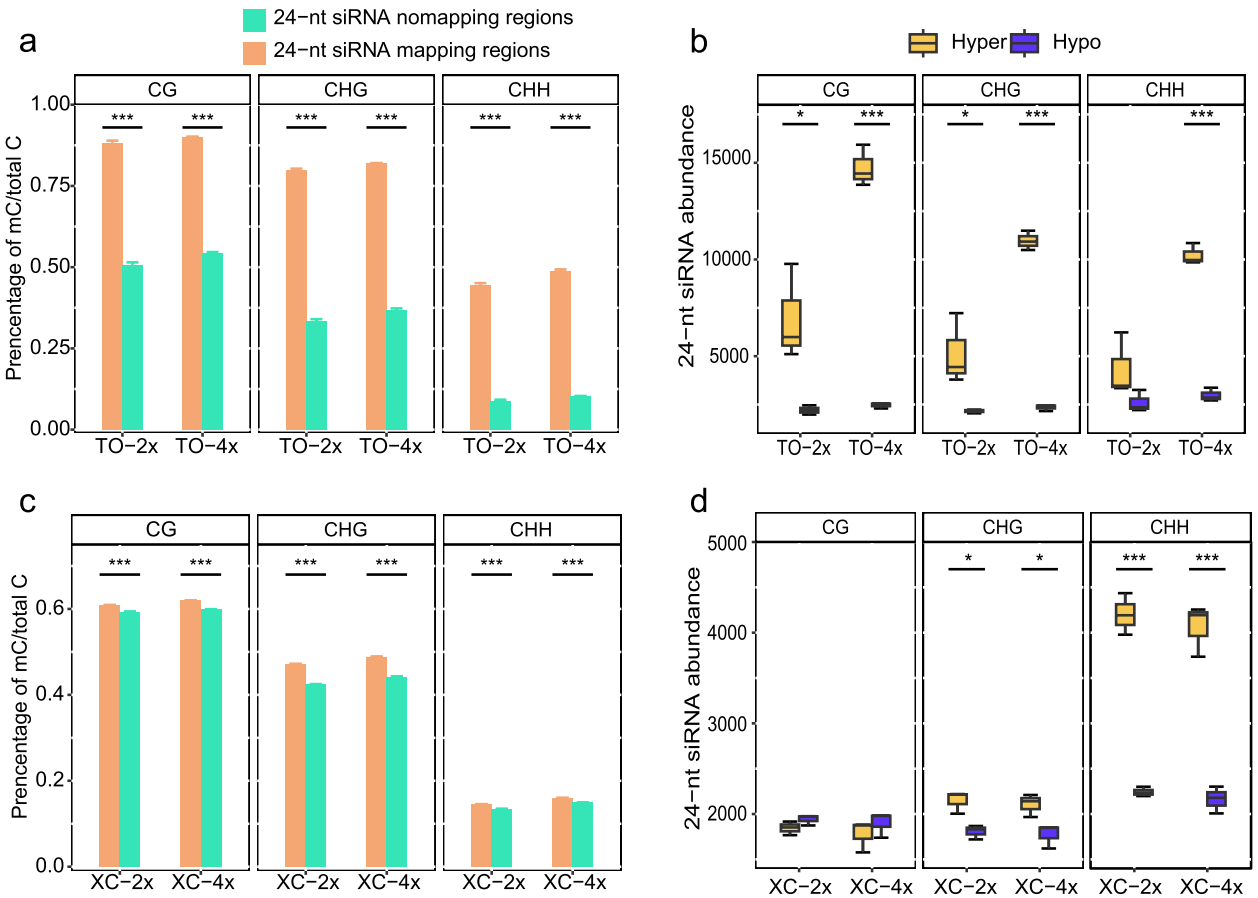


Fig. 8 DNA methylation levels and 24-nucleotide siRNA abundances. Comparison of DNA methylation levels in regions mapped by 24-nt siRNAs with those without 24-nt siRNAs in TO (**a**) and XC (**c**). Abundance of 24-nt siRNAs in CG, CHG, and CHH hyper- and hypomethylated regions in tetraploid (4X) compared to diploid (2X) in TO (**b**) and XC (**d**). Error bars represent standard deviations, $n = 3$ (*P-value < 0.05, ***P-value < 0.001, two-way ANOVA). XC: Ziyang Xiangcheng (*Citrus junos Sieb.* ex Tanaka); TO: Trifoliate orange (*Poncirus trifoliata* L. Raf.)

crucial role in modulating DNA methylation changes during citrus genome duplication.

Discussion

DNA methylation is partially responsible for gene expression variations in citrus tetraploids

Polyploidy has been a critical driver in the evolution of angiosperms (Jiao et al. 2011, Leitch and Leitch 2008, Wendel et al. 2016). In this study, genome-wide bisulfite sequencing was employed to compare DNA methylation patterns between diploid and tetraploid forms of two citrus genotypes, XC and TO. A correlation between methylation patterns and genomic regions was identified (Zhang et al. 2015), with many DMRs located in intergenic areas (Fig. 4c). DNA methylation can suppress gene expression by obstructing transcription factor binding at promoters or altering transposon activity (Zhang et al. 2018). Typically, 24-nt siRNAs generated from repetitive or intergenic regions guide the RdDM pathway to induce sequence-specific DNA methylation (Castel and Martienssen 2013, Simon and Meyers 2011). Analysis of small RNA profiles confirmed the dominance of 24-nt siRNAs in citrus leaves (Figure S12). In TO, tetraploids exhibited a significantly higher abundance of 24-nt siRNAs than diploids, and regions associated with these siRNAs showed markedly increased methylation compared to those without (Fig. 8a, c). Thus, siRNAs contribute to methylation changes driven by variations in citrus ploidy.

However, alterations in DNA methylation are not always directly correlated with changes in gene expression. Other factors, including chromatin structure, transcription factor accessibility, and non-coding RNA regulation, also influence gene expression (Ausin et al. 2016, Li et al. 2012). More than half of the 70 genes overlapping between DMGs and DEGs exhibited an inverse relationship between methylation levels and gene expression (Figure S10). Studies in Arabidopsis polyploids suggest that DNA methylation accounts for only a small fraction of gene expression variability (Meng et al. 2016). In citrus, as in other plant polyploids, DNA methylation appears to explain only part of the gene expression changes observed during polyploidization.

DNA methylation-associated gene expression changes may contribute to morphological variations in citrus tetraploids

Tetraploid XC and TO exhibit typical polyploid morphological traits, including reduced stature, enlarged and thickened leaves, and larger stomata with decreased density (Tan et al. 2015, 2017). In tetraploid citrus leaves, both leaf size and mesophyll cell wall thickness were significantly increased compared to their diploid counterparts (Fig. 1a). Polyploids generally display larger organs, such as leaves, flowers, and seeds, relative to diploids (Bomblies 2020). These phenotypic differences may be linked to the methylation status of genes involved in cell wall formation, suggesting that WGD-induced DNA methylation changes are associated with enhanced cell wall development in citrus tetraploids (Figure S4, S7).

Analysis of DNA methylation and gene expression revealed a set of genes exhibiting both differential methylation and expression in XC and TO, particularly those involved in plant growth and stress resistance. Notably, the *ACN1* (*Pt9g001570*) gene, linked to stomatal size and drought tolerance, the *NAC036* (*Pt8g000730*) gene, associated with plant height and drought resistance, the *ASMT* (*Cs6g_pb003480*) gene, related to salt tolerance, and the *BG1* (*Pt9g014360*) gene, which modulates plant growth and stress response by elevating ABA levels, were identified (Dong et al. 2018, Kato et al. 2010, Liu et al. 2022, Zheng et al. 2017). These genes may play a critical role in the phenotypic differences between citrus diploids and tetraploids and represent promising targets for further research into the molecular mechanisms underlying altered polyploid traits.

The differentially methylated genes (DMGs) may contribute to wider adaptability of citrus tetraploids

In tetraploids, DMGs were significantly enriched in pathways related to immune response, salicylic acid response, stimulus and defense responses, fatty acid response, and jasmonic acid response (Fig. 5a, c, e). It is well established that polyploidization enhances plants' adaptability to diverse environmental conditions. For instance, tetraploidization in rice induces DNA hypomethylation, activating genomic loci associated with stress-response genes involved in signaling pathways and jasmonate production, thereby facilitating rapid and robust stress responses (Wang et al. 2021a). Similarly, tetraploid apples exhibit greater resistance to apple scab (*Venturia inaequalis*) compared to diploids (Hias et al. 2018). In citrus tetraploids, DMGs enriched in jasmonic acid-related processes may contribute to increased environmental adaptability.

Polyploidization in citrus also leads to elevated levels of primary metabolites, such as sucrose, proline, and gamma-aminobutyric acid (GABA), alongside a reduction in secondary metabolites like flavanones, phenylpropanoids, and terpenoids (Tan et al. 2015, 2017). The observed metabolic shifts in citrus tetraploids may be driven by DNA methylation changes in key genes. For example, among the hypermethylated genes, *CsTT7* encodes a flavonoid 3'-hydroxylase involved in flavonoid biosynthesis (Han et al. 2010), while *CsCYP83B1* encodes an oxime-metabolizing enzyme critical in the biosynthetic pathway of glucosinolates, potentially influencing

apical development (Naur et al. 2003). Mapman analysis revealed that DMGs were particularly enriched in the synthesis and degradation of phenylpropanoids and in ROS-related pathways (Figure S4-S9). These polyploidization-induced DNA methylation changes likely underpin alterations in phenylpropanoid metabolism and ROS responses, both of which play vital roles in plant stress resilience.

Conclusions

In this study, transcriptome analysis and WGBS were employed to examine two pairs of citrus tetraploids and their diploid counterparts. The tetraploid citrus plants exhibited reduced CG methylation within both gene bodies and TE bodies compared to diploids. DMGs between tetraploid and diploid plants were enriched in pathways related to immune response, organ development, metabolism, and secondary metabolite production. Despite these differences, only 150 and 58 DEGs were identified between the tetraploid and diploid samples of TO and XC, respectively. Notably, *ACN1*, *NAC036*, and *ASMT1* were among the 70 genes displaying both altered DNA methylation and expression, providing valuable insight into the regulatory mechanisms associated with polyploidization.

Supplementary Information

The online version contains supplementary material available at https://doi.org/10.1007/s44281-024-00051-6.

Additional file 1: Figure S1. Global methylome maps of TO. A: Genome of TO, B: gene density, C: TE density, D: TO-2x-CG density, E: TO-2x-CHG density, F: TO-2x-CHH density, G: TO-4x-CG density, H: TO-4x-CHG density, I: TO-4x-CHH density. TO: Trifoliate orange.

Additional file 2: Figure S2. Global methylome maps of XC. A: Genome of XC, B: gene density, C: TE density, D: XC-2x-CG density, E: XC-2x-CHG density, F: XC-2x-CHH density, G: XC-4x-CG density, H: XC-4x-CHG density, I: XC-4x-CHH density. XC: Ziyang Xiangcheng.

Additional file 3: Figure S3. KEGG functional enrichment of DMGs between diploids and tetraploids. The top 15 enriched pathways are shown. KEGG functional enrichment of CG-DMGs (A), CHG-DMGs (B), and CHH-DMGs (C) between XC-2x and XC-4x. D. Venn diagrams display the overlap between DMGs in the three contexts and DEGs in XC (D). E. KEGG functional enrichment of CG-DMGs (D), CHG-DMGs (E), CHH-DMGs (F) between TO-2x and TO-4x. XC: Ziyang Xiangcheng; TO: Trifoliate orange.

Additional file 4: Figure S4. Mapman analysis of XC-DMGs (Metabolism_overview).

Additional file 5: Figure S5. Mapman analysis of XC-DMGs (Secondary Metabolism).

Additional file 6: Figure S6. Mapman analysis of XC-DMGs (Cellular_response_overview).

Additional file 7: Figure S7. Mapman analysis of TO-DMGs (Metabolism_overview).

Additional file 8: Figure S8. Mapman analysis of TO-DMGs (Secondary Metabolism).

Additional file 9: Figure S9. Mapman analysis of TO-DMGs (Cellular_response_overview).

Additional file 10: Figure S10. DMG&DEG heatmap of TO (A) and XC (B).

Additional file 11: Figure S11. RT-qPCR of differentially expressed genes (DEGs) and BS-PCR of PtACN1. **a**: Transcript levels of six selected DEGs, as revealed by RT-qPCR (bars) and RNA-seq (green lines). **b**: DNA methylation levels of PtACN1, as revealed by BS-PCR (blue bar represents the percentage of mC/total C) and WGBS (green bar represents DNA methylation level).

Additional file 12: Figure S12. Small RNA distribution.

Additional file 13: Table S1 Primers for BS-PCR and RT-PCR. Table S2 Cell Wall thickness (μm) of diploid and autotetraploid. Table S3 Details of the bisulfite sequencing libraries generated in diploid and tetraploid. Table S4 Percentages of methylated cytosines (mCs). Table S5 Ratios of mCs in CG, CHG and CHH contexts. Table S6 Comparison of methylation levels in genic and transposable element (TE) regions between diploid and autotetraploid. Table S7 Categories and numbers of TEs. Table S8 Number of differentially hypermethylated and hypomethylated regions. Table S9 The proportions of DMRs overlapped with TEs. Table S10 Distribution of differentially methylated regions at different locations in the genome.

Acknowledgments
Not applicable.

Authors' contributions
W.W.G. and X.M.W. conceived and designed the project; H.G. performed the experiments and analyzed the data with contributions from G.A.X. and Y.B.; K.D.X. and Q.M.X. prepared the materials; H.G. wrote the manuscript with contributions from X.M.W. and W.W.G.

Funding
This research was financially supported by grants from the National Key Research & Development Program of China (no. 2023YFD1200103), the National Natural Science Foundation of China (nos. 32172525, 32202432), the China Agriculture Research System (no. CARS-26) and the Natural Science Foundation of Hubei Province (no. 2022CFB675).

Availability of data and materials
The raw data that support the findings of this study are openly available in NGDC database under the BioProject accession number PRJCA024899.

Declarations

Ethics approval and consent to participate
Not applicable.

Consent for publication
Not applicable.

Competing interests
The authors declare that they have no competing interests.

Received: 3 April 2024 Revised: 6 August 2024 Accepted: 7 August 2024
Published online: 10 November 2024

References

Aleza P, Froelicher Y, Schwarz S, Agustí M, Hernández M, Juárez J, et al. Tetraploidization events by chromosome doubling of nucellar cells are frequent in apomictic citrus and are dependent on genotype and environment. Ann Bot. 2011;108:37–50. https://doi.org/10.1093/aob/mcr099.

Allario T, Brumos J, Colmenero-Flores J, Tadeo F, Froelicher Y, Talon M, et al. Large changes in anatomy and physiology between diploid Rangpur lime (*Citrus limonia*) and its autotetraploid are not associated with large

changes in leaf gene expression. J Exp Bot. 2011;62:2507–19. https://doi.org/10.1093/jxb/erq467.
Ausin I, Feng S, Yu C, Liu W, Kuo H, Jacobsen EL, et al. DNA methylome of the 20-gigabase norway spruce genome. Proc Natl Acad Sci USA. 2016;113:E8106–13. https://doi.org/10.1073/pnas.1618019113.
Bolger AM, Lohse M, Usadel B. Trimmomatic: a flexible trimmer for Illumina sequence data. Bioinformatics. 2014;30:2114–20. https://doi.org/10.1093/bioinformatics/btu170.
Bomblies K. When everything changes at once: finding a new normal after genome duplication. Proc Biol Sci. 2020;287:20202154. https://doi.org/10.1098/rspb.2020.2154.
Bu D, Luo H, Huo P, Wang Z, Zhang S, He Z, et al. KOBAS-i: intelligent prioritization and exploratory visualization of biological functions for gene enrichment analysis. Nucleic Acids Res. 2021;49:W317–25. https://doi.org/10.1093/nar/gkab447.
Castel SE, Martienssen RA. RNA interference in the nucleus: roles for small RNAs in transcription, epigenetics and beyond. Nat Rev Genet. 2013;14:100–12. https://doi.org/10.1038/nrg3355.
Comai L. The advantages and disadvantages of being polyploid. Nat Rev Genet. 2005;6:836–46. https://doi.org/10.1038/nrg1711.
Dobin A, Davis CA, Schlesinger F, Drenkow J, Zaleski C, Jha S, et al. STAR: ultrafast universal RNA-seq aligner. Bioinformatics. 2013;29:15–21. https://doi.org/10.1093/bioinformatics/bts635.
Dong H, Bai L, Zhang Y, Zhang G, Mao Y, Min L, et al. Modulation of guard cell turgor and drought tolerance by a peroxisomal acetate–malate shunt. Mol Plant. 2018;11:1278–91. https://doi.org/10.1016/j.molp.2018.07.008.
Finnegan E, Peacock W, Dennis E. DNA methylation, a key regulator of plant development and other processes. Curr Opin Genet Dev. 2000;10:217–23. https://doi.org/10.1016/S0959-437X(00)00061-7.
Guo W, Fiziev P, Yan W, Cokus S, Sun X, Zhang MQ, et al. BS-Seeker2: a versatile aligning pipeline for bisulfite sequencing data. BMC Genomics. 2013;14:774. https://doi.org/10.1186/1471-2164-14-774.
Guo W, Zhu P, Pellegrini M, Zhang MQ, Wang X, Ni Z. CGmapTools improves the precision of heterozygous SNV calls and supports allele-specific methylation detection and visualization in bisulfite-sequencing data. Bioinformatics. 2018;34:381–7. https://doi.org/10.1093/bioinformatics/btx595.
Han Y, Vimolmangkang S, Soria-Guerra RE, Rosales-Mendoza S, Zheng D, Lygin AV, et al. Ectopic expression of apple *F3'H* genes contributes to anthocyanin accumulation in the Arabidopsis *tt7* mutant grown under nitrogen stress. Plant Physiol. 2010;153:806–20. https://doi.org/10.1104/pp.109.152801.
Hias N, Svara A, Keulemans J. Effect of polyploidisation on the response of apple (Malus × domestica Borkh.) to Venturia inaequalis infection. Eur J Plant Pathol. 2018;151:515–26. https://doi.org/10.1007/s10658-017-1395-2.
Huang Y, Xu Y, Jiang X, Yu H, Jia H, Tan C, et al. Genome of a citrus rootstock and global DNA demethylation caused by heterografting. Hortic Res. 2021;8:69. https://doi.org/10.1038/s41438-021-00505-2.
Ibarra C, Feng X, Schoft V, Hsieh T, Uzawa R, Rodrigues J, et al. Active DNA demethylation in plant companion cells reinforces transposon methylation in gametes. Science. 2012;337:1360–4. https://doi.org/10.1126/science.1224839.
Jiao Y, Wickett NJ, Ayyampalayam S, Chanderbali AS, Landherr L, Ralph PE, et al. Ancestral polyploidy in seed plants and angiosperms. Nature. 2011;473:97–100. https://doi.org/10.1038/nature09916.
Kanehisa M, Araki M, Goto S, Hattori M, Hirakawa M, Itoh M, et al. KEGG for linking genomes to life and the environment. Nucleic Acids Res. 2008;36:D480–4. https://doi.org/10.1093/nar/gkm882.
Kato H, Motomura T, Komeda Y, Saito T, Kato A. Overexpression of the NAC transcription factor family gene *ANAC036* results in a dwarf phenotype in *Arabidopsis thaliana*. J Plant Physiol. 2010;167:571–7. https://doi.org/10.1016/j.jplph.2009.11.004.
Lavania UC, Srivastava S, Lavania S, Basu S, Misra NK, Mukai Y. Autopolyploidy differentially influences body size in plants, but facilitates enhanced accumulation of secondary metabolites, causing increased cytosine methylation. Plant J. 2012;71:539–49. https://doi.org/10.1111/j.1365-313X.2012.05006.x.
Leitch AR, Leitch IJ. Genomic plasticity and the diversity of polyploid plants. Science. 2008;320:481–3. https://doi.org/10.1126/science.1153585.
Li E, Beard C, Jaenisch R. Role for DNA methylation in genomic imprinting. Nature. 1993;366:362–5. https://doi.org/10.1038/366362a0.
Li G, Chen C, Chen P, Meyers B, Xia R. sRNAminer: A multifunctional toolkit for next-generation sequencing small RNA data mining in plants. Sci Bull. 2024;69:784–91.https://doi.org/10.1016/j.scib.2023.12.049.
Li X, Zhu J, Hu F, Ge S, Ye M, Xiang H, et al. Single-base resolution maps of cultivated and wild rice methylomes and regulatory roles of DNA methylation in plant gene expression. BMC Genomics. 2012;13:300. https://doi.org/10.1186/1471-2164-13-300.
Liang W, Xie K, Guo D, Xie Z, Yi H, Guo W. Spontaneous generation and SSR molecular characterization of autotetraploids in ten citrus rootstocks. J Fruit Sci. 2014;31:1–6.
Liao Y, Smyth GK, Shi W. FeatureCounts: an efficient general purpose program for assigning sequence reads to genomic features. Bioinformatics. 2014;30:923–30. https://doi.org/10.1093/bioinformatics/btt656.
Liu WC, Song RF, Zheng SQ, Li TT, Zhang BL, Gao X, et al. Coordination of plant growth and abiotic stress responses by tryptophan synthase beta subunit 1 through modulation of tryptophan and ABA homeostasis in *Arabidopsis*. Mol Plant. 2022;15:973–90. https://doi.org/10.1016/j.molp.2022.04.009.
Love MI, Huber W, Anders S. Moderated estimation of fold change and dispersion for RNA-seq data with DESeq2. Genome Biol. 2014;15:550. https://doi.org/10.1186/s13059-014-0550-8.
Matzke MA, Mosher RA. RNA-directed DNA methylation: an epigenetic pathway of increasing complexity. Nat Rev Genet. 2014;15:394–408. https://doi.org/10.1038/nrg3683.
Meng D, Dubin M, Zhang P, Osborne E, Stegle O, Clark R, et al. Limited contribution of DNA methylation variation to expression regulation in Arabidopsis thaliana. PLoS Genet. 2016;12:e1006141.https://doi.org/10.1371/journal.pgen.1006141.
Naur P, Petersen BL, Mikkelsen MD, Bak S, Rasmussen H, Olsen CE, et al. CYP83A1 and CYP83B1, two nonredundant cytochrome P450 enzymes metabolizing oximes in the biosynthesis of glucosinolates in Arabidopsis. Plant Physiol. 2003;133:63–72. https://doi.org/10.1104/pp.102.019240.
Pooggin M. How can plant DNA viruses evade siRNA-directed DNA methylation and silencing?. Int J Mol Sci. 2013;14:15233–59. https://doi.org/10.3390/ijms140815233.
Rival A, Ilbert P, Labeyrie A, Torres E, Doulbeau S, Personne A, et al. Variations in genomic DNA methylation during the long-term in vitro proliferation of oil palm embryogenic suspension cultures. Plant Cell Rep. 2013;32:359–68. https://doi.org/10.1007/s00299-012-1369-y.
Saleh B, Allario T, Dambier D, Ollitrault P, Morillon R. Tetraploid citrus rootstocks are more tolerant to salt stress than diploid. C R Biol. 2008;331:703–10. https://doi.org/10.1016/j.crvi.2008.06.007.
Simon SA, Meyers BC. Small RNA-mediated epigenetic modifications in plants. Curr Opin Plant Biol. 2011;14:148–55. https://doi.org/10.1016/j.pbi.2010.11.007.
Soltis DE, Visger CJ, Soltis PS. The polyploidy revolution then… and now: stebbins revisited. Am J Bot. 2014;101:1057–78. https://doi.org/10.3732/ajb.1400178.
Tan FQ, Tu H, Liang WJ, Long JM, Wu XM, Zhang HY, et al. Comparative metabolic and transcriptional analysis of a doubled diploid and its diploid citrus rootstock (C. junos cv. Ziyang xiangcheng) suggests its potential value for stress resistance improvement. BMC Plant Biol. 2015;15:89. https://doi.org/10.1186/s12870-015-0450-4.
Tan FQ, Tu H, Wang R, Wu XM, Xie KD, Chen JJ, et al. Metabolic adaptation following genome doubling in citrus doubled diploids revealed by non-targeted metabolomics. Metabolomics. 2017;13:143. https://doi.org/10.1007/s11306-017-1276-x.
Wang L, Cao S, Wang P, Lu K, Song Q, Zhao FJ, et al. DNA hypomethylation in tetraploid rice potentiates stress-responsive gene expression for salt tolerance. Proc Natl Acad Sci USA. 2021a;118:e2023981118. https://doi.org/10.1073/pnas.2023981118.
Wang L, Huang Y, Liu Z, He J, Jiang X, He F, et al. Somatic variations led to the selection of acidic and acidless orange cultivars. Nat Plants. 2021b;7:954–65. https://doi.org/10.1038/s41477-021-00941-x.
Wang Y, Zuo L, Wei T, Zhang Y, Zhang Y, Ming R, et al. CHH methylation of genes associated with fatty acid and jasmonate biosynthesis contributes to cold tolerance in autotetraploids of *Poncirus trifoliata*. J Integr Plant Biol. 2022;64:2327–43. https://doi.org/10.1111/jipb.13379.
Wei T, Wang Y, Xie Z, Guo D, Chen C, Fan Q, et al. Enhanced ROS scavenging and sugar accumulation contribute to drought tolerance of naturally

occurring autotetraploids in *Poncirus trifoliata*. Plant Biotechnol J. 2019;17:1394–407. https://doi.org/10.1111/pbi.13064.
Wendel JF, Jackson SA, Meyers BC, Wing RA. Evolution of plant genome architecture. Genome Biol. 2016;17:37. https://doi.org/10.1186/s13059-016-0908-1.
Xia QM, Miao LK, Xie KD, Yin ZP, Wu XM, Chen CL, et al. Localization and characterization of *Citrus* centromeres by combining half-tetrad analysis and CenH3-associated sequence profiling. Plant Cell Rep. 2020;39:1609–22. https://doi.org/10.1007/s00299-020-02587-z.
Xu Q, Chen LL, Ruan X, Chen D, Zhu A, Chen C, et al. The draft genome of sweet orange (*Citrus sinensis*). Nat Genet. 2013;45:59–66. https://doi.org/10.1038/ng.2472.
Zhang J, Liu Y, Xia EH, Yao QY, Liu XD, Gao LZ. Autotetraploid rice methylome analysis reveals methylation variation of transposable elements and their effects on gene expression. Proc Natl Acad Sci USA. 2015;112:E7022–9. https://doi.org/10.1073/pnas.1515170112.
Zhang H, Lang Z, Zhu JK. Dynamics and function of DNA methylation in plants. Nat Rev Mol Cell Biol. 2018;19:489–506. https://doi.org/10.1038/s41580-018-0016-z.
Zheng X, Tan D, Allan AC, Zuo B, Zhao Y, Reiter RJ, et al. Chloroplastic biosynthesis of melatonin and its involvement in protection of plants from salt stress. Sci Rep. 2017;7:41236. https://doi.org/10.1038/srep41236.

Publisher's Note

Springer Nature remains neutral with regard to jurisdictional claims in published maps and institutional affiliations.